The British Journal of Radiology, 84 (2011), 5–18

REVIEW ARTICLE

The corpus callosum: white matter or terra incognita

[1]A FITSIORI, [2]D NGUYEN, [3]A KARENTZOS, [2]J DELAVELLE and [2]M I VARGAS

[1]*Department of Radiology and* [2]*Department of Neuroradiology, Geneva University Hospital University of Geneva, Geneva, Switzerland, and* [3]*Hatzikosta General Hospital of Ioannina, Ioannina, Greece*

ABSTRACT. The corpus callosum is the largest white matter structure in the brain, consisting of 200–250 million contralateral axonal projections and the major commissural pathway connecting the hemispheres of the human brain. The pathology of the corpus callosum includes a wide variety of entities that arise from different causes such as congenital, inflammatory, tumoural, degenerative, infectious, metabolic, traumatic, vascular and toxic agents. The corpus callosum, or a specific part of it, can be affected selectively. Numerous pathologies of the corpus callosum are encountered during CT and MRI. The aim of this study is to facilitate a better understanding and thus treatment of the pathological entities of the corpus callosum by categorising them according to their causes and their manifestations in MR and CT imaging. Familiarity with its anatomy and pathology is important to the radiologist in order to recognise its disease at an early stage and help the clinician establish the optimal therapeutic approach.

Received 25 January 2010
Accepted 3 March 2010

DOI: 10.1259/bjr/21946513

The corpus callosum (CC), situated in the centre of the human brain, forms the largest commissural white matter bundle in the brain. Therefore, its role is essential to the integration of the information between left and right cerebral hemispheres.

Anatomy of the CC has gained new interest in recent years owing to an increasing number of callosotomies performed to treat intraventricular lesions, as well as for the treatment of certain forms of generalised epilepsy [1]. Furthermore, development of new techniques in MRI, such as diffusion tensor imaging (DTI), as well as evolution of older techniques permitting high-resolution imaging of the human brain, has enhanced interest in the study of specific brain structures and their correlation to clinical syndromes.

Despite its essential role in interhemispheric communication, there are only a few studies concerning the CC. As a result, up until now, the CC remains a relatively unexplored region of the brain, somewhat of a ''terra incognita'' for the radiologist. Early cartographers claimed that fantastic beasts existed in remote corners of the world and depicted such as decoration on their maps. Although no beasts are to be found at the CC, there are indeed quite a few pathological entities affecting this structure of the human brain. Modern imaging modalities enable their thorough ''exploration'' and accurate mapping. Our study focuses on the description of the different pathologies affecting this structure of the human brain and their radiological manifestations.

Address correspondence to: Dr Maria Isabel Vargas, Department of Neuroradiology, Geneva University Hospital, 4 Rue Gabrielle-Perret-Gentil, 1211 Geneva 14, Switzerland. E-mail: maria.i.vargas@hcuge.ch

Disclosure: The authors report no conflicts of interest.

Technique

In this paper we review the normal anatomy of the CC with conventional and new techniques (DTI) followed by the description and illustration of its commonest pathologies encountered during routine CT and MRI in our institute. CT and MR images were obtained with a 16- or 64-detector multislice Philips (Phillips Achieva, Eindhoven, the Netherlands) CT device and a 1.5 T or 3 T Siemens (Siemans, Erlangen, Germany) or Philips MRI device, respectively. In addition to the usual morphological MRI sequences, a sagittal T_1 or T_2 (fluid-attenuated inversion recovery (FLAIR)) weighted plane, as well as DTI reformatting images for an optimal study of the CC, were implemented.

MRI is the modality of choice for the study of the CC. As a densely packed white matter structure, the CC is visualised with a high signal in T_1 weighted imaging (WI) and a low signal in T_2 images. Sagittal plane images provide an overview of the structural integrity and extent of development of the CC, whereas in coronal images we can better evaluate its relationship to the cerebral hemispheres.

Complete assessment of CC pathologies is facilitated by the acquisition of the following sequences: T_1 WI, fast spin-echo (FSE) T_2 WI, as well as FLAIR sequences and volume acquisition sequences with high resolution.

New techniques such as DTI have further expanded our capability to visualise the organisation and orientation of the axonal pathways of the CC with tractography and quantitatively with the use of anisotropic indices of diffusion such as fraction anisotropy (FA) maps, permitting a better comprehension and analysis of the CC microstructure.

The use of susceptibility-sensitive sequences (susceptibility-weighting imaging (SWI)) plays an important role in the assessment of traumatic injury and other pathologies of the brain resulting in the deposition of blood products or calcium, including pathologies affecting the CC. Vascular (three-dimensional (3D) time-of-flight (TOF)) sequences, on the other hand, are essential in cases of ischaemic or haemorrhagic lesions.

Images after contrast media enhancement are not necessary for the study of malformations or traumatic pathologies of the CC.

If a viral infection is suspected, the MRI study, including perfusion sequences, should be repeated within 48–72 h after the initial study in order to confirm the diagnosis.

CT imaging is important for the diagnosis of CC lipomas and other pathologies with calcium deposition and can also be useful for the diagnosis of tumour, haemorrhage or infarction; CT angiography is essential for the diagnosis of aneurysms responsible for haematomas, more commonly situated in the anterior part of the CC.

Normal anatomy of the corpus callosum

The CC is the largest commissural pathway consisting of a cross-sectional area representing twice the magnitude of the sum of all the other commissural structures in the brain of an adult [1]. It consists of myelinated axons that cross the midline in the developing brain in order to connect homologous regions of the two hemispheres.

Four named regions are described by anatomists for the CC. These are anteriorly to posteriorly the rostrum, the genu, the body and the splenium (Figures 1–3).

Embryology of the CC is not yet well known. Rakic and Yakovlev [2], who studied the development of the commissures, and Griffiths et al [3], who studied the normal anatomy of the CC in children and its anatomical variations, support the cranial/caudal direction in its developmental process, with the pioneering fibres of the future CC crossing the midline at 12–13 weeks

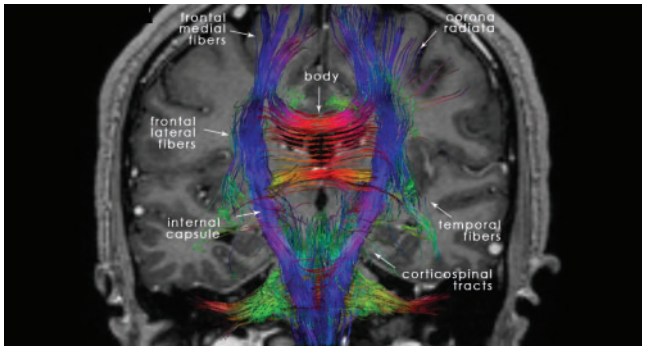

Figure 2. 22-year-old normal participant: coronal tractography depicting the anatomy of the different fibres and connections of the corpus callosum (CC) as a part of the corticospinal tracts, as well as its associations with the other cerebral structures.

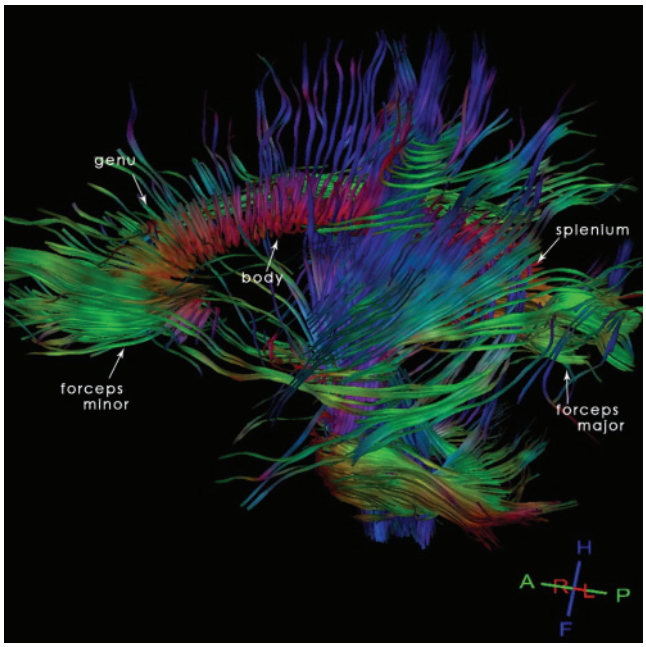

Figure 1. 22-year-old normal participant: sagittal tractography reconstruction allowing a representation of the organisation and orientation of the axonal pathways of the corpus callosum (CC) and demonstrating the different anatomical regions of the CC.

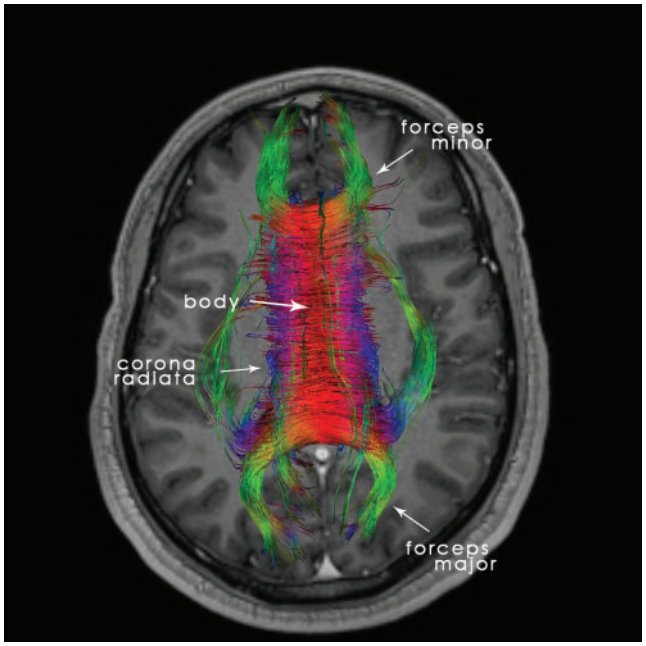

Figure 3. 22-year-old normal participant: axial tractography reconstruction, helpful for the comprehension and analysis of the corpus callosum (CC)'s microstructure.

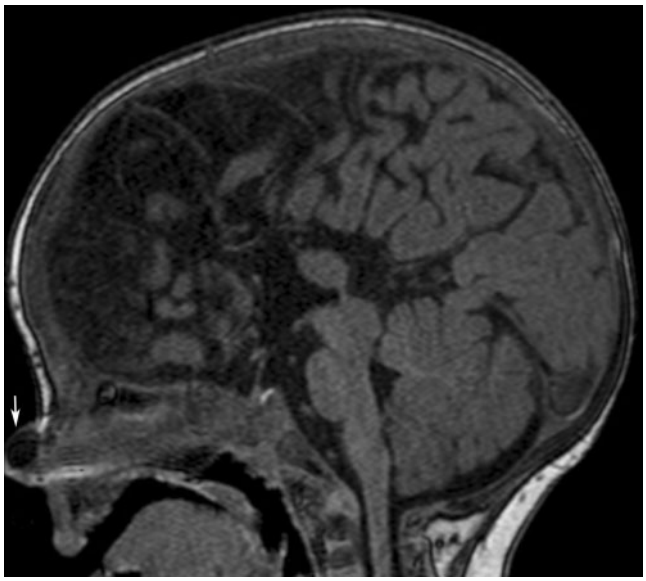

(a)

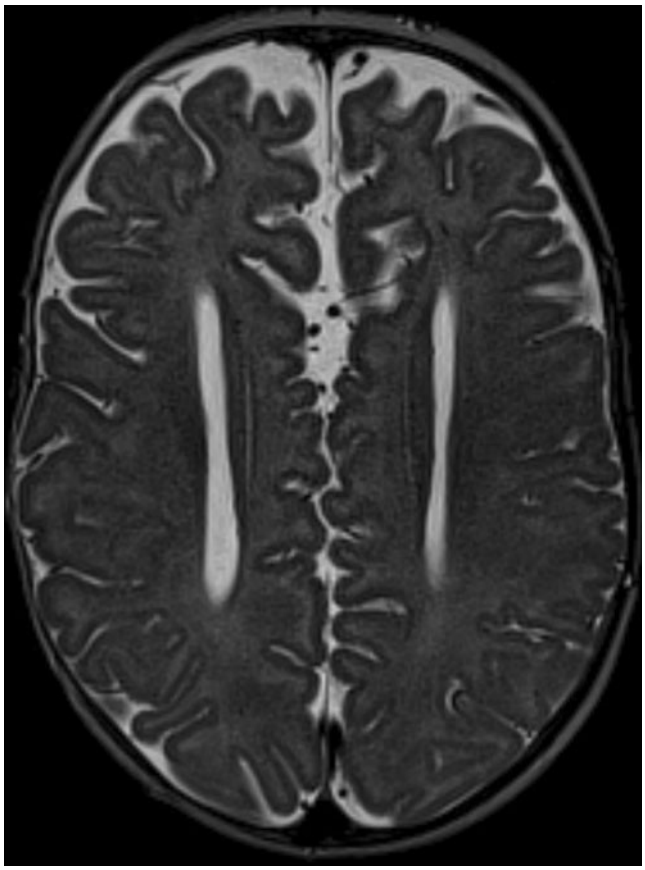

(b)

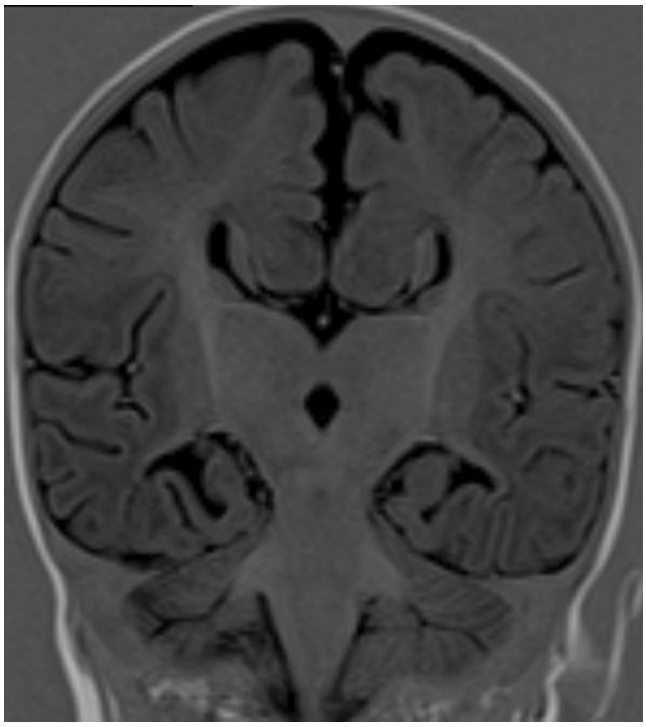

(c)

Figure 4. 6-year-old boy with corpus callosum (CC) agenesis: in the sagittal plane in MRI there is no structure consistent with the CC present in its usual location (a); a dermoid cyst of the nose associated with this malformation is observed (arrow). MR axial image: parallel lateral ventricles and ''B bundles of Probst'' (b). MR coronal image: ''trident'' anterior horns resembling ''Viking helmet'' or ''mouse head'' (c).

post-conceptional age. Other scientists support the theory that the CC's development is progressing in the opposite direction (caudally to cranially) and some recent studies propose a more complex pattern. The development is completed within the first 4 years of life and a reduction in the CC's size is observed after 40 years of age.

The fibres of the genu are crossing over to contribute to the forceps minor, connecting the homologous lateral and medial regions of the frontal cortices, whereas the fibres of the splenium follow a posterior course contributing to the forceps major, connecting the occipital lobes (Figure 2). The body fibres are directed towards the cerebral cortex on a traversal axis to form the corona radiata along with other major white matter pathways. Finally, the rostral fibres are connecting the orbital regions of the frontal lobes. Nowadays, we can easily map the course of the CC's fibres with the use of the DTI technique, which permits a virtual 3D visualisation of the white matter.

The CC is intimately related to the fornix and the lateral ventricles and represents the anterior, superior and posterior border of the septum pellicidum, which together with the fornix separate the lateral ventricles from each other. The fornix itself forms the inferior border of the septum pellicidum. The tapetum, consisting of the body's and the splenium's fibres, is lying across the body and the postero-inferior part of the ventricles (Figure 3).

The arterial supply of the CC is provided by the internal carotid artery system, with the pericallosal artery (branch of the anterior cerebral artery) with the exception of the splenium, which is vascularised by the terminal and choroidal branches of the posterior cerebral artery (vertebrobasilar system). The carotid system also contributes to the CC's arterial supply by the anterior communicating artery, which gives off an inconstant artery, called median artery of the CC. [4].

Venous drainage is facilitated by the callosal and callosal cingular veins towards the internal cerebral veins [5].

Congenital pathology

The congenital pathology of the CC includes agenesis or hypoplasia and the CC's lipomas.

The least significant form of hypoplasia of the CC is the absence of the rostrum. It is rarely of major clinical significance and is usually an incidental finding in MRI for other reasons.

CC agenesis (Figure 4a–c) is one of the more frequent congenital malformations with a prevalence of 3–7 per 1000 births. Its diagnosis can be made with the use of antenatal ultrasound and it can be associated with other midline malformations (cavum septum pellicidum, cavum vergae, etc.), as well as malformations of the posterior fossa or the cerebral cortex. It can be either asymptomatic or associated with psychomotor retardation, epilepsy or psychiatric syndromes [6]. It can be part of Aicardi syndrome, Andermann syndrome and Apert syndrome. Aetiologies include genetics (trisomies 8, 13, 18), metabolic causes, drugs (cocaine) or viral infection (influenza) [7].

MRI manifestation is characteristic:

- axial images: parallel lateral ventricles and ''B bundles of Probst '' in DTI; and
- coronal images: ''trident'' anterior horns resembling ''Viking helmet'' or ''mouse head''.

Rokitansky initially described CC lipomas (Figure 5) in 1856 [8]. They are considered to be congenital malformations of the primitive meninx and can be asymptomatic in 40% of cases. When symptomatic, they are associated with headaches, epilepsy and motor dysfunction.

They are classified as curvilinear or tubulonodular [9]. Curvilinear lipomas are usually situated in the posterior part of the CC and are asymptomatic, whereas the tubulonodular lipomas are usually found in the anterior part and are associated with severe frontal malformations [10]. Their CT and MRI presentation is characteristic: highly hypodense in CT images, hyperintense in T_1 MR images and iso- or hypointense in T_2 MR images. Fat-suppression techniques are useful for confirmation with MRI. There is no feasible surgical treatment because of the vascular and neural structures present inside the lesion.

Ischaemic pathology

CC ischaemia is not very common and this is attributed to its rich supply from three main arterial systems: the anterior communicating artery, the anterior pericallosal artery and the posterior cerebral artery. Ischaemia can be the result of emboli, stenosis due to atheromatosis or vasospasm of the anterior or posterior cerebral arteries and their branches. CC infarction due to cerebral venous thrombosis has also been reported [11] as a rare condition.

The MRI manifestation of CC ischaemia is common in all cases with an increased signal in diffusion-weighted images (DWI) and a corresponding decreased signal in the apparent diffusion coefficient (ADC) map until day 4 when the ADC reaches normal values. Enhancement after contrast media administration is usually apparent

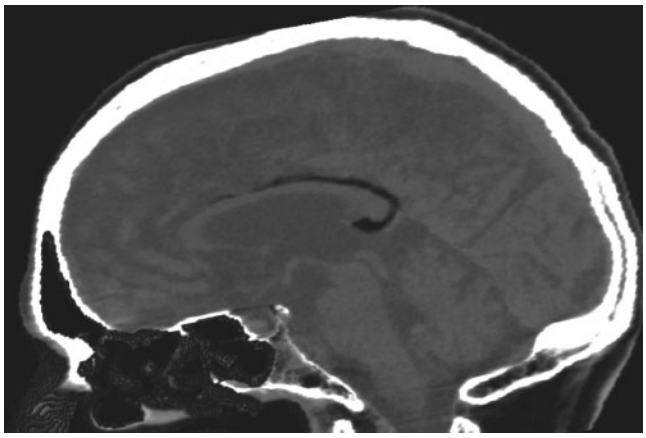

Figure 5. 68-year-old man with a lipoma in the posterior part of the corpus callosum body. CT presentation is characteristic: the lesion is highly hypodense in non-contrast CT images.

after day 7, consistent with rupture of the haemato-encephalic barrier. In FSE T_2 weighting and FLAIR sequences a high signal can be observed after 8–12 h.

If ischaemia of the splenium is suspected, then the homolaterous thalamus and the mesial-posterior region of the temporal lobe are also ischaemic (Figure 6) because of pathology (emboli, stenosis) of the homolateral posterior cerebral artery. In cases of ischaemia of the anterior part of the CC, ischaemia of the anterior cerebral territory is usually also present.

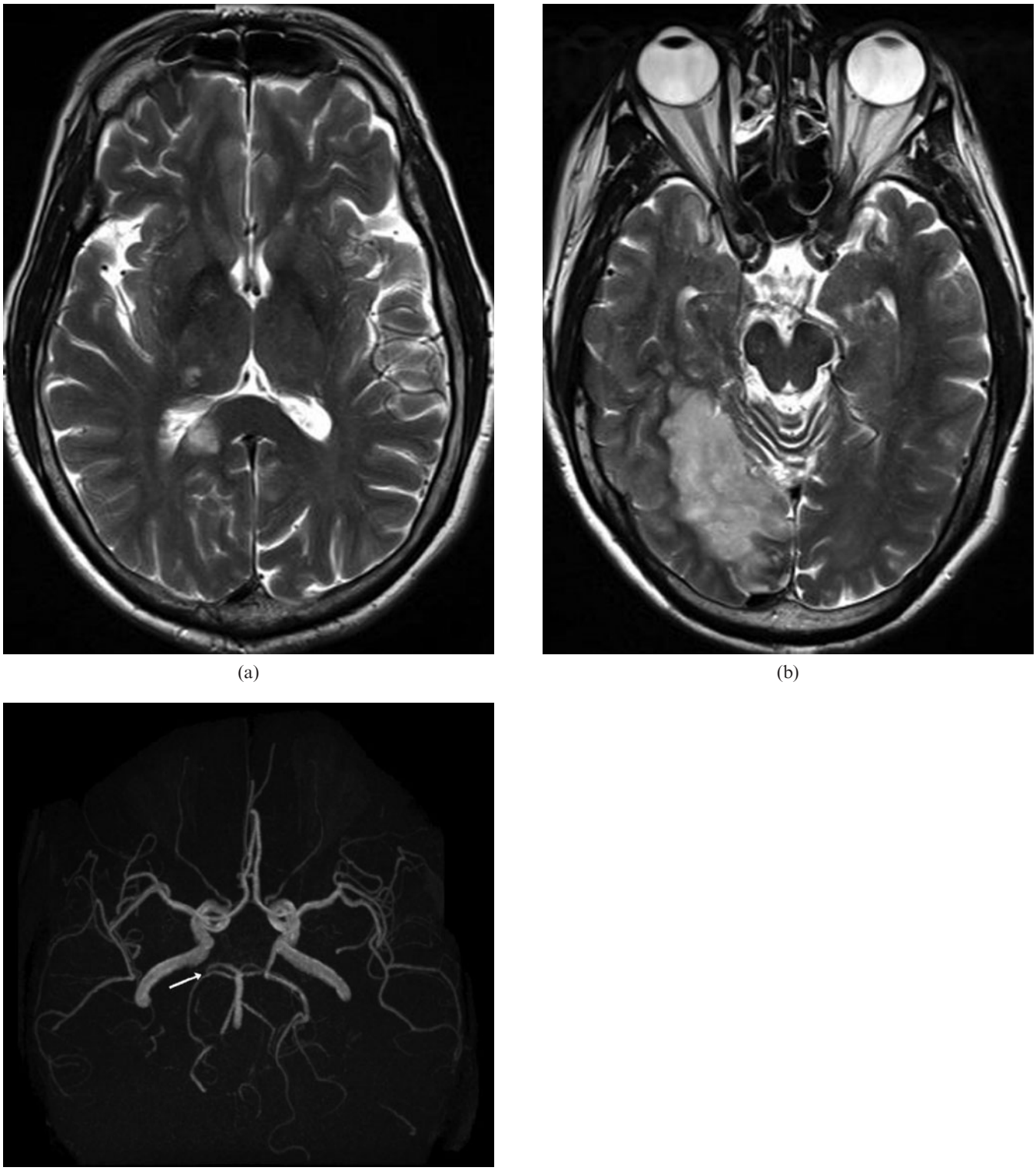

(a) (b) (c)

Figure 6. 53-year-old man with ischaemia: MRI showing ischaemia of the right part of the splenium (a), homolateral thalamus and the mesial-posterior region of the temporal lobe (b), because of emboli in the proximal right posterior cerebral artery, well demonstrated in the three-dimensional time-of-flight sequence (c, arrow).

CC infarcts may present atypical clinical and radiological findings that are more suggestive of tumour. Appropriate imaging studies, including DWI, perfusion imaging, spectroscopy, as well as follow-up studies can be useful to avoid unnecessary biopsies [12].

Haemorrhagic pathology

Ruptured aneurysms of the anterior cerebral artery or the pericallosal artery are usually the cause of CC haemorrhage (Figure 7). This is why all cases of

(a)

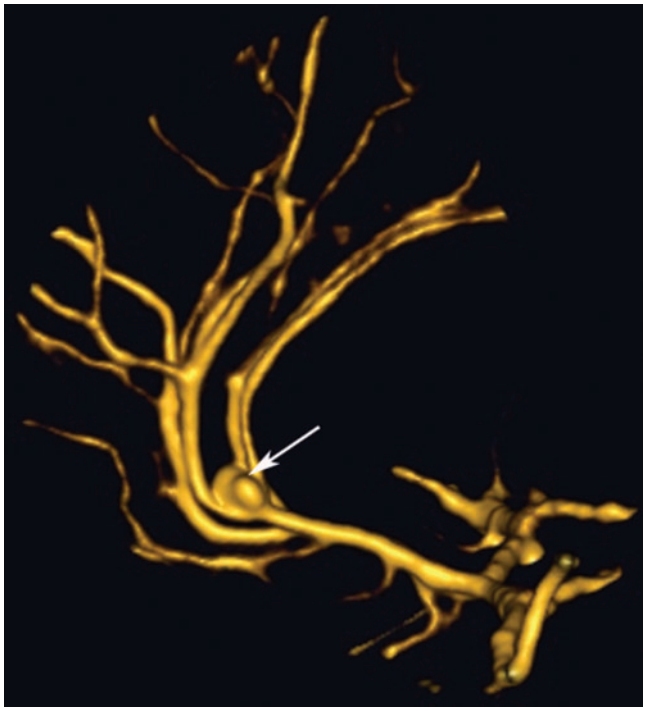

(b)

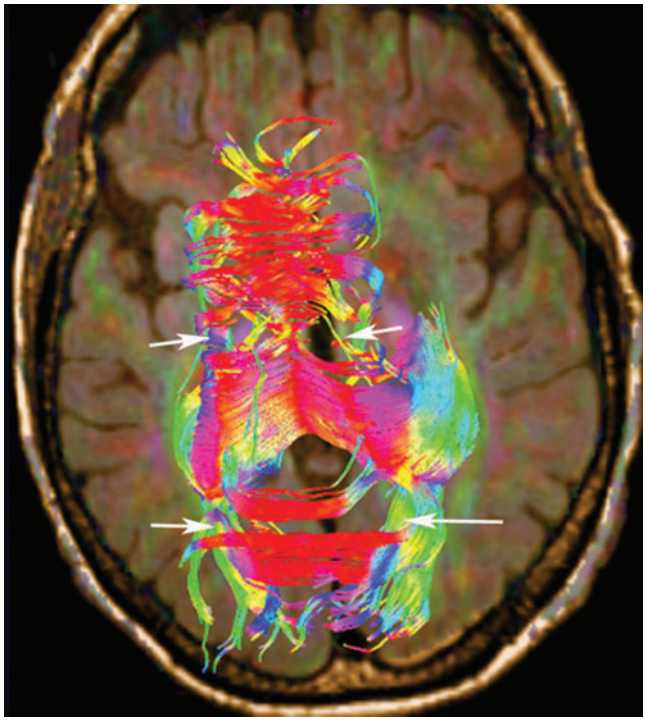

(c)

Figure 7. 60-year-old woman with aneurysm of the anterior communicating artery; hyperdensity in the region of the corpus callosum (CC) in non-contrast CT axial images corresponds to a haematoma (a, arrows). (b) Three-dimensional time-of-flight MRI sequence showing aneurysm of the anterior communicating artery (arrow). (c) The tractography reconstruction demonstrating the rarefaction of the fibres of the CC associated with the lesion (arrows).

haematomas situated in the anterior part of the CC should be studied by CT angiography or 3D TOF MRI sequences.

CC haemorrhage can also be associated with ventriculostomies, especially in patients with coagulation problems.

Other less frequent aetiologies include isolated cavernomas of the CC or microhaemorrhages occurring in severe, non-lethal high-altitude cerebral oedema [13]. In addition to the conventional T_2* MRI sequence, highly sensitive SWI is very useful in these rare cases.

Toxic pathology

Marchiafava–Bignami (MB) is a rare toxic disease, mostly seen in chronic alcoholism, that results in acute demyelination and necrosis of the CC [14, 15]. The disease typically affects the body of the CC, followed by the genu and finally the splenium. Other white matter tracts such as the anterior and posterior commissures and the corticospinal tracts may be involved (Figure 8). Lesions can also be found in the hemispheric white matter and in the middle cerebellar peduncles.

Patients present with acute mental confusion, disorientation, neurocognitive deficits and seizures. Most patients presenting with the acute type of MB will go into a coma and eventually die. Patients with the subacute type of MB, which is characterised by dementia, dysarthria and muscle hypertonia, may survive for years. The chronic form of MB is characterised by chronic dementia, with astasia–abasia, dysarthria and sometimes signs of interhemispheric disconnection.

In MRI, patients with MB show areas of low T_1 signal intensity and high T_2 and FLAIR signal intensity with predominance in the splenium and the genu. In DWI an increased signal can be seen with a corresponding decreased signal in the ADC map. These lesions do not invoke mass effect and may show peripheral contrast enhancement during the acute phase. Eventually, the lesions cavitate and become well marginated. They are difficult to visualise on CT scans, where they appear as hypoattenuated areas, located mainly in the genu and the splenium. Regression of the lesions associated with favourable clinical evolution has been reported.

Clinically silent lesions of the splenium of the CC of patients receiving anti-epileptic treatment have been reported, as well as CC lesions associated with rapid

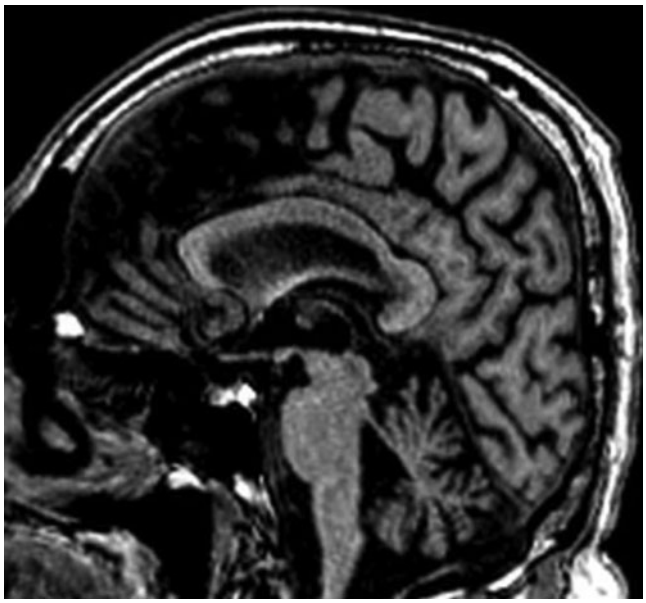

(a)

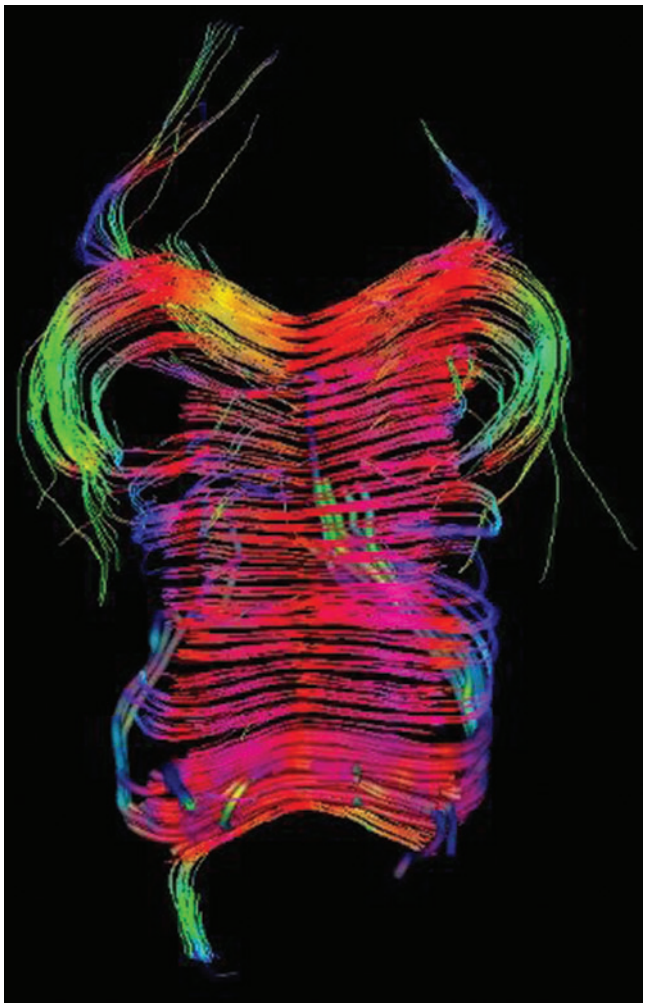

(b)

Figure 8. 63-year-old man with Marchiafava–Bignami disease. MRI shows areas of low T_1 signal intensity (a), at the level of the corpus callosum (CC) splenium, with rarefaction of the CC fibres on tractography (b).

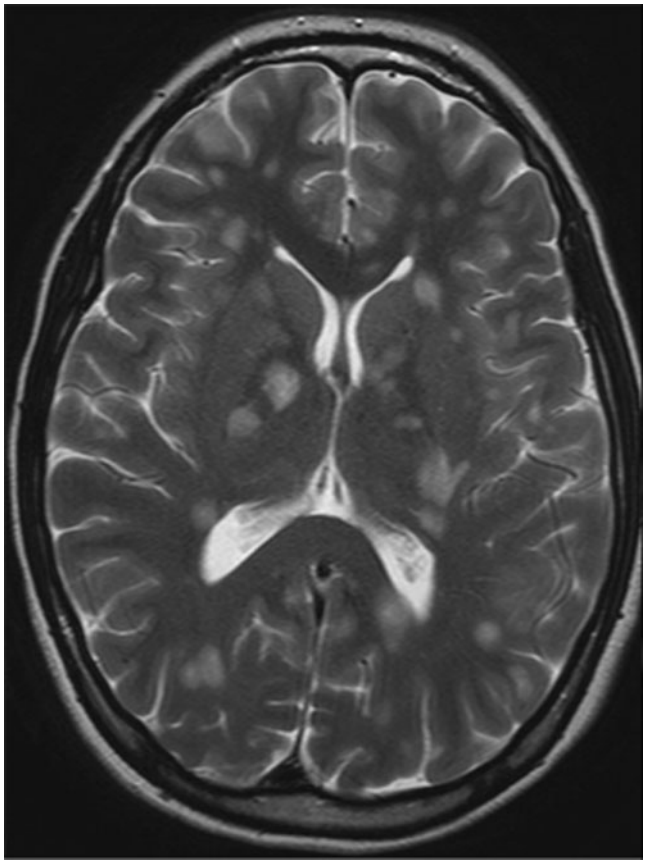

(a)

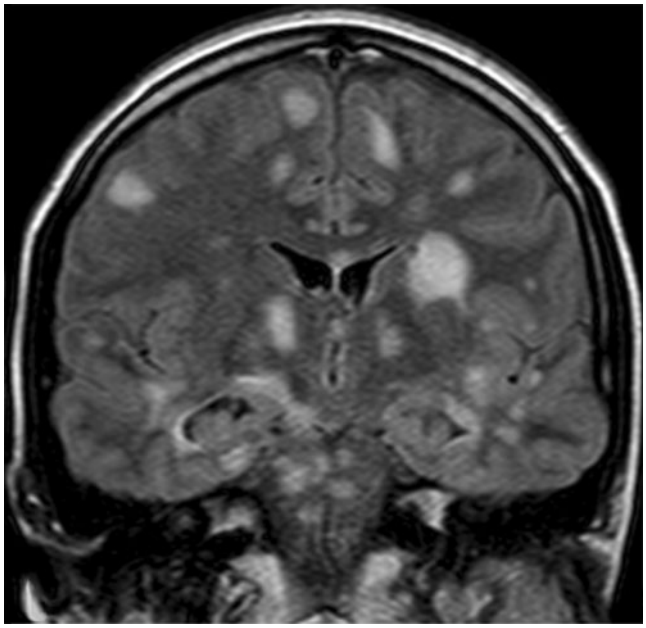

(b)

(c)

Figure 9. 25-year-old woman with multiple sclerosis: MRI illustrates clearly demyelinating lesions in the periventricular, cortical, internal capsule, corpus callosum and spinal cord regions; hyperintense on T_2 weighted image (a) and fluid-attenuated inversion recovery (b) with enhancement in T_1 weighted image (c, arrows).

withdrawal from anti-epileptic drugs (AEDs). The latter are benign, clinically silent and can be completely reversible in a period of 1 month without any treatment required. The main pathophysiological hypothesis proposes an intramyelinic oedema, possibly induced by abrupt AED concentration changes, which is consistent with the integrity of neuronal fibres in DTI, as well as with the reversible character of the lesions [16]. Direct toxicity induced by AED seems unlikely, given the poor prevalence of the observed lesions in the epilepsy patient population receiving AED. MRI findings also include a high signal in FSE T_2 and FLAIR images, as well as a restriction of diffusion, located in the CC's splenium.

The abuse of drugs such as cocaine and heroin has also been blamed for the formation of lesions in the splenium of the CC. Cocaine abuse has been linked to intramyelinic oedema as well as mitochondrial dysfunction. Heroin is suspected to cause neurovascular toxicity.

In acute carbon monoxide (CO) intoxication, patients may develop progressive white matter demyelinisation [17]. This damage is variable and ranges from discrete perivascular foci in the CC to axonal destruction. This process can lead to disconnection syndrome and severe dysfunction of the neurocognitive networks, apparent in a late phase. Imaging findings are considered non-sensitive for assessing the clinical consequences of neurotoxicity in these patients and usually appear later than the clinical symptoms. Conventional MRI is not specific, including high signal in T_2 and FLAIR sequences as well as a restriction of diffusion, although Lin et al [17] consider that DTI is a useful tool for studying this type of pathology. They have shown that fractional anisotropy is decreased in the CC and in the white matter in the fronto-orbital, parietal and temporal regions of patients suffering from CO intoxication compared with healthy participants, which explains the delayed cognitive symptoms.

Infectious pathology

Potentially reversible lesions of the CC splenium related to viral infections have been described in children and in adults [18]. The viruses more commonly related to CC lesions are HSV-6, influenza virus, Epstein–Barr virus, papovirus JC and others.

The pathophysiology of these lesions is not yet well known. It is believed that viruses can cause intramyelinic oedema.

MRI characteristics in these cases are high T_2 signal, slightly low or no particular signal in T_1 imaging, with a restriction of diffusion and a decreased ADC. No vascular anomaly in vascular sequences is observed to be associated with the lesions.

If a viral infection is suspected, a new MRI study after 48–72 h is necessary: disappearance of the signal abnormalities confirms the diagnosis.

More extensive and severe lesions can be associated with bacterial infections causing encephalitis, abscesses

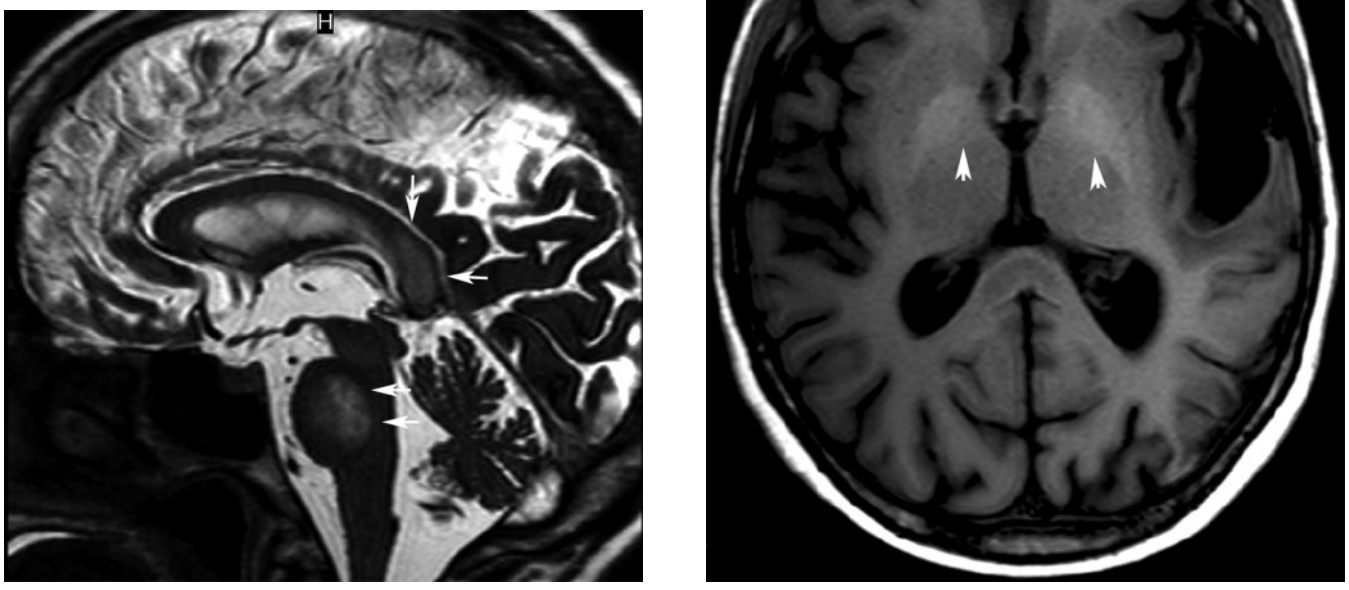

(a) (b)

Figure 10. 47-year-old woman with known history of alcohol abuse presenting central pontine and extrapontine myelinolysis, attributed to rapid correction of hyponatraemia. MRI shows high signal in T_2 images and low signal in T_1 images at the level of the pons and the corpus callosum splenium (a and b, respectively), associated with spontaneously high signal in the globus pallidus (b, arrows) on T_1 weighted images without contrast-media enhancement.

or mycotic aneurysms. Patients usually suffer from endocarditis or bacteraemia and the germs found include *Staphylococcus aureus*, *Escherichia coli* and *Salmonella enteritidis*.

Inflammatory pathology

Multiple sclerosis (MS) is the principal pathology affecting the CC and the pericallosal region.

The lesions related to MS are well studied and described. They present a high signal in T_2 or FLAIR imaging, isointense or hypointense in T_1 weighting and can be enhanced after contrast administration depending on their activity. Sagittal plane images are very useful in evaluating the morphology, size and severity of the lesions (Figure 9).

Acute disseminated encephalomyelitis (ADEM) is a rare demyelinating disease that affects the central

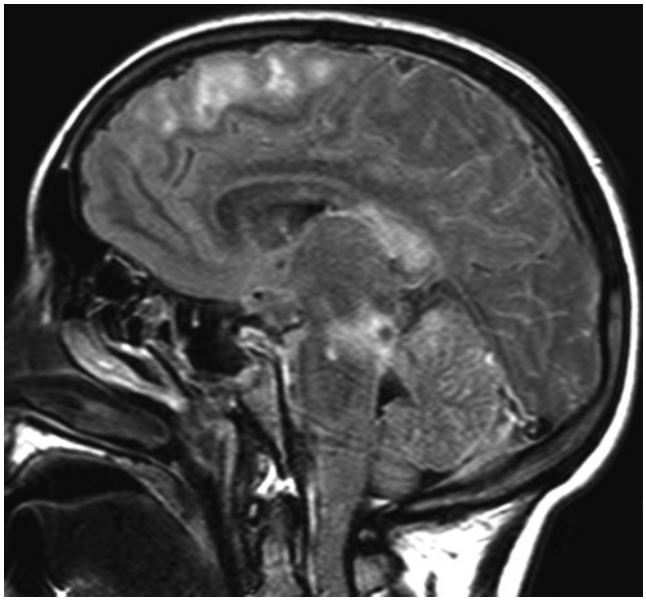

(a)

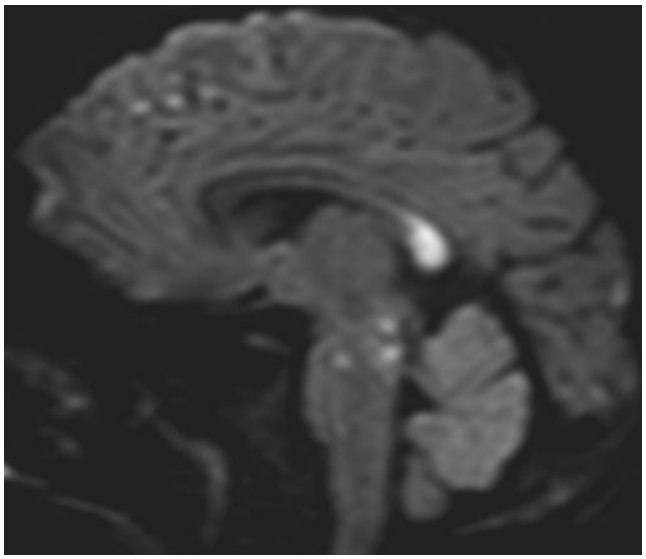

(b)

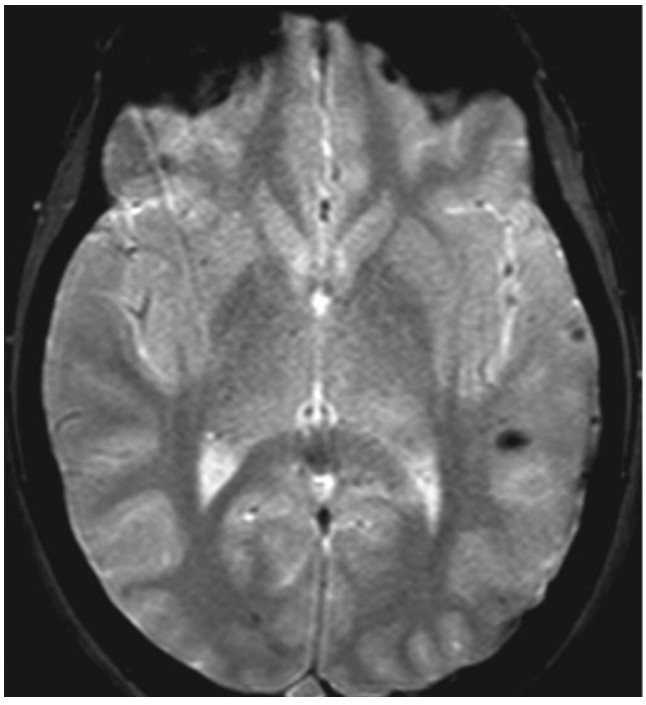

(c)

Figure 11. 19-year-old girl (ski accident): MRI study shows multiple hyperintense lesions in fluid-attenuated inversion recovery sequences (a) associated with a restriction of diffusion (b) and microhaemorrhages (c) at the level of the posterior part of the corpus callosum, the mesencephalon, and the cortical and subcortical frontal and temporal regions, respectively (a–c), consistent with diffuse axonal injury.

nervous system (CNS) in a multifocal way owing to an immune system failure. It affects men and women equally, but more frequently children and adolescents, and it usually appears after viral infection or vaccination.

Clinical manifestation varies depending on the regions affected: seizures, headaches, coma, cerebellar syndrome or disconnection syndrome can be present, usually surfacing 1–3 weeks after vaccination or infection. If the spinal cord is affected, paraparesis, tetraparesis or paraplegia can be present.

MRI presentation is not specific. Therefore, clinical correlation is very important for the diagnosis if the patient has a definite history of neurological symptoms following infection and pathological lumbar puncture findings. Multiple hyperintense lesions in T_2 and FLAIR imaging affecting the supratentorial white matter, the basal ganglia, the mesencephalon, the pons and the cerebellum, associated or not with an enhancement after contrast media administration, are present in the demyelinated regions [19]. MRI findings can be present late after the appearance of symptoms.

Metabolic pathology

MRI findings in hypoglycaemic brain pathology typically describe lesions involving the CC, basal ganglia and hippocampus. Transient hypoglycaemic encephalopathy has been reported as a rare cause of reversible lesions of the CC splenium [20]. A DWI abnormality characterised by high signals in the CC splenium with corresponding ADC reductions, completely reversed within 1–2 days following appropriate correction of hypoglycaemia, can be observed. No residual lesion is present in T_2 or FLAIR images and MR angiography shows associated no vascular lesion.

Acute hydrocephalus can be responsible for CC distension, which is visible as a thin aspect of the CC in MRI according to some authors [21], whereas others [22] correlate a central pontine and extrapontine myelinolysis due to hyperglycaemia.

Central pontine myelinolysis is also associated with rapid correction of hyponatraemia [23, 24]. In 10% of cases extrapontine myelinolysis coexists, and in these cases the CC splenium can be affected (Figure 10). The pathophysiology of the lesions involves osmotic demyelination. Hyponatraemia is usually observed in patients with a history of alcohol abuse, diabetes mellitus, renal failure, malnutrition or cancer and receiving chemotherapy. MRI findings include high signal in T_2 and FLAIR sequences, slightly low signal in T_1 WI, a restriction of diffusion in the acute phase, an enhancement after contrast media administration in the subacute phase and a high signal in ADC maps in the subacute and chronic phases [24].

Traumatic pathology

Diffuse axonal injury (DAI) is a common consequence of traumatic brain injury (TBI) that frequently involves the parasagittal white matter, CC and brain stem [25].

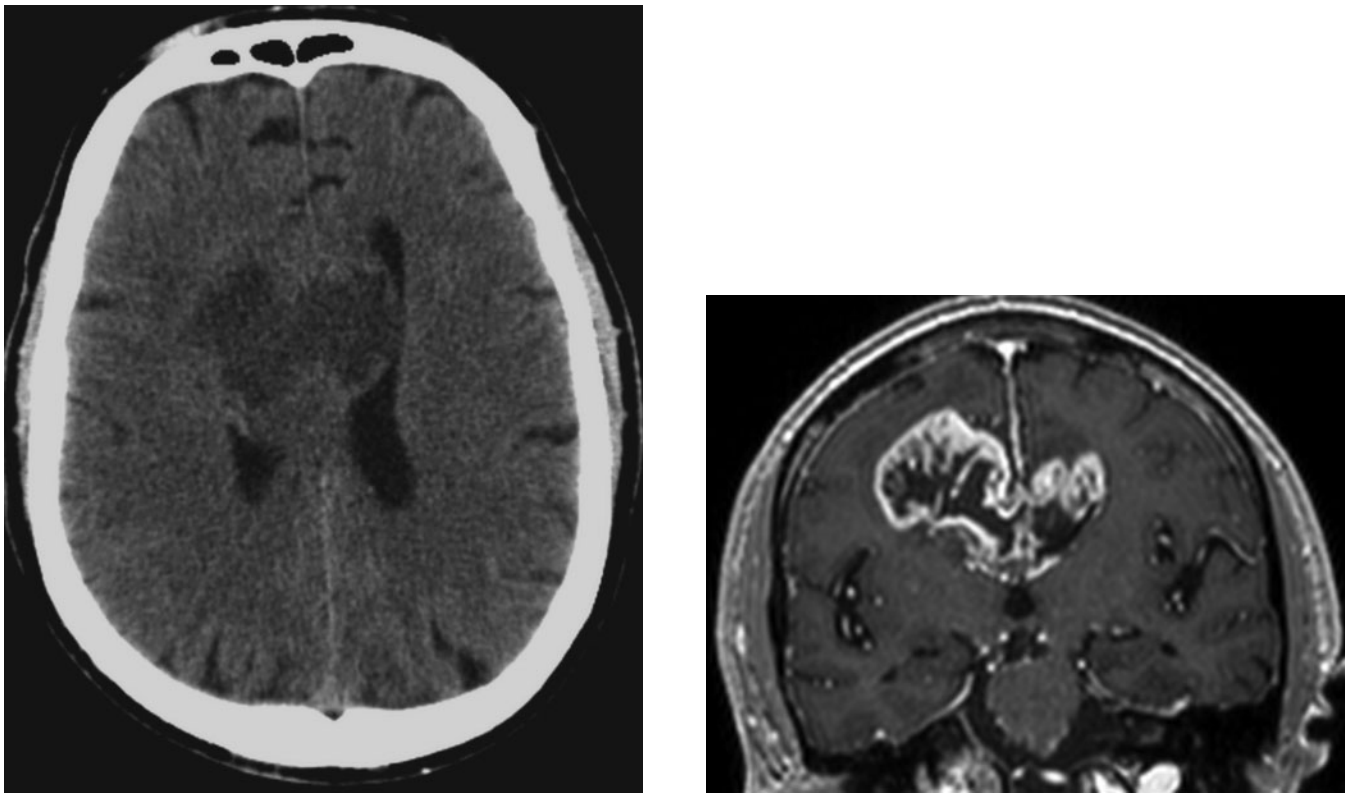

(a) (b)

Figure 12. 64-year-old woman with glioblastoma: non-contrast CT scan shows a hypodense mass in the corpus callosum (a). The lesion in MRI T_1 weighted image after contrast media presents annular irregular enhancement around a necrotic lesion (b).

DAI results from sustained acceleration–deceleration forces that can shear axons and produce microscopic changes in the brain (Figure 11).

CT and MRI studies have shown that the CC is unevenly affected in TBI in the sense that the splenium and posterior part of the CC are more commonly affected (56% and 80%) [26]. The proposed mechanism to explain this finding focuses on the closer anatomical relationship of the falx to the posterior part of the CC, which limits lateral movement of the hemispheres in the posterior region, resulting in concentration of the strain in the posterior part of the CC during brain injury. In addition, the CC is easily distorted at its thinnest part, which is the body–splenium junction. Other mechanisms described involve laceration of the upper surface of the CC by the end of the falx, sudden increase in the intraventricular pressure and stretching of the CC.

The most common CC lesions found in TBI are microhaemorrhages. This is the reason why T_2* and DWI sequences are indispensable in studies suggesting DAI or traumatic CC lesions.

In FLAIR or spin-echo (SE) T_2 images, hyperintense regions can be found, with a moderate correlation with long-term functional outcome as measured by the Glasgow Outcome Scale Extended (GOSE), according to the study of Marquez de la Plata et al [27].

DTI has evolved in recent years to be a valuable tool for the investigation of the integrity of CC fibres after head injury and the evaluation of CC atrophy secondary to cortical or subcortical lesions resulting from a TBI.

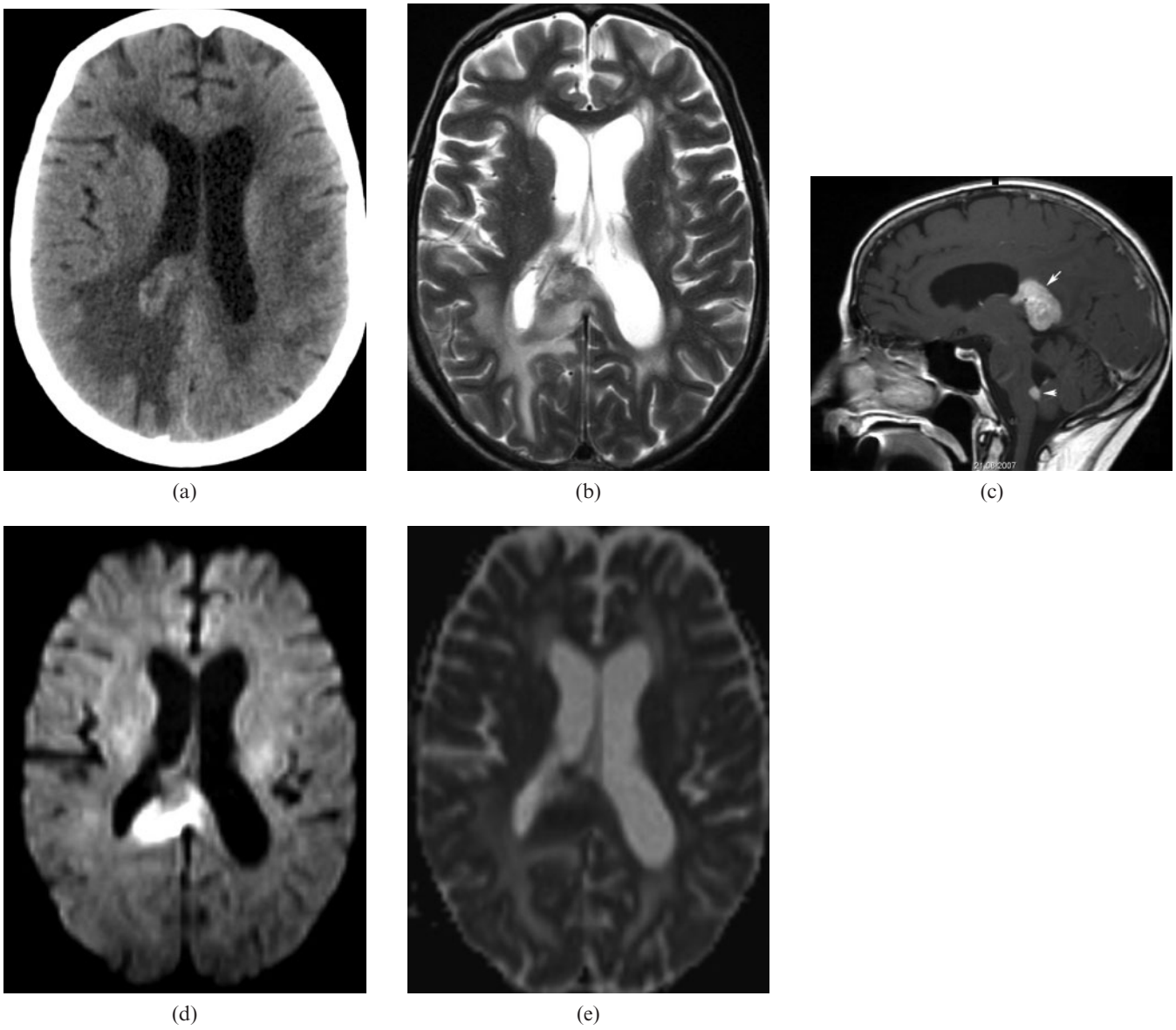

Figure 13. 66-year-old woman with lymphoma: non-contrast CT scan showing a spontaneously hyperdense mass at the corpus callosum (CC) splenium surrounded by extensive oedema (a). MRI is hyperintense in T_2 images (b), with homogeneous enhancement at the CC splenium and the inferior part of the fourth ventricle (c, arrows). In diffusion weighted images (d, e) there is a restriction of diffusion enabling differential diagnosis from glioblastoma. A lesion with the same characteristics is also present in the brain stem as seen in the sagittal plane.

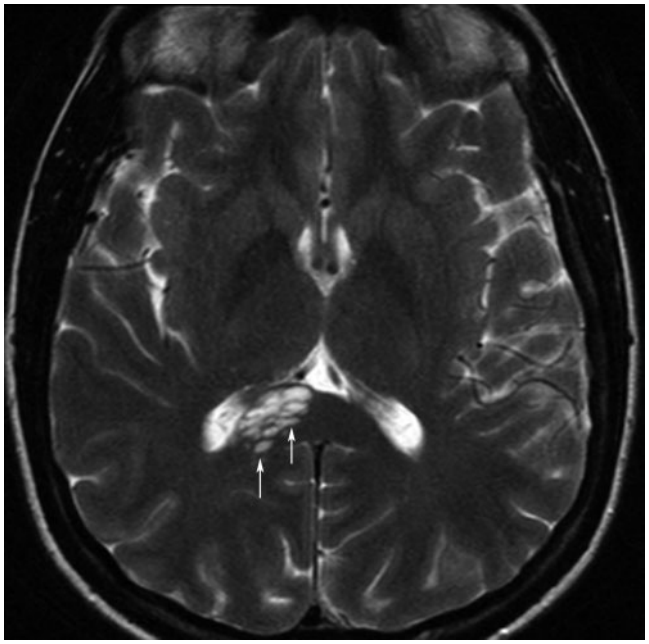

Figure 14. 51-year-old woman with many dilated Virchow–Robin spaces (arrows) in the right part of the corpus callosum splenium resulting in a cystic appearance.

Fibre tracking algorithms can be used to reconstruct white matter fibres in 3D and better demonstrate these lesions [28].

Tumoural pathology

The tumoural pathology more commonly found in the CC includes glioblastomas, lymphomas and metastases.

Glioblastomas (Figure 12) are the commonest among astrocytomas, representing 50–60% of all. They frequently affect the population between 45 and 70 years of age. Characterised by a rapid growing rate, with central necrosis and neovascularisation, they usually have a poor prognosis.

MRI is the modality of choice for their study: in T_2 WI, FLAIR imaging glioblastomas are usually heterogeneous and hyperintense, in T_1 WI isointense or hypointense, and there is no restriction of diffusion in DWI. Cystic lesions or haemorrhage inside the lesion can be observed, and after contrast media administration there is usually an annular irregular enhancement around a necrotic lesion. In spectroscopy there is a decrease in *N*-acetylaspartate (NAA), an increase in choline and a peak in lactates and lipids.

Differential diagnosis (DD) includes lymphoma, metastases, subacute ischaemia and tumefactive demyelinating disease.

Primitive cerebral lymphomas represent 1–7% of all brain tumours. They are usually non-Hodgkin B-cell tumours and in recent years have been observed mostly in patients with a suppressed immune system or immunodeficiencies [29].

In CT imaging, lymphoma can be hyperdense (Figure 13) in non-contrast images with a strong enhancement after contrast media administration.

In MR images, it shows high signal in T_2 and FLAIR sequences, low signal in T_1 sequences and homogeneous enhancement after contrast media administration (Figure 12) in immunocompetent patients, whereas in patients with immunodeficiencies the enhancement is annular with central necrosis. In DWI there is a restriction that helps with DD from glioblastoma. Another key to the lymphoma diagnosis is its profound localisation in proximity to the ventricles and the CC.

DD includes glioblastoma, toxoplasmosis, cerebral abscess and progressive multifocal leukoencephalopathy.

Cerebral metastases usually have the imaging characteristics of the primary tumour.

Iatrogenic pathology

Prolongated ventricular drainage can result in CC dilacerations and ventriculostomies in CC haemorrhage, especially in patients with coagulation problems.

Miscellaneous pathology

CC atrophy can be the result of cortical and subocortical hemispheric lesions due to ischaemic parenchymal destruction, traumatic lesions, degenerative diseases or periventricular leukomalacia.

High-altitude cerebral oedema (HACE) usually occurs in non-acclimatised individuals exposed rapidly to high altitudes (up to 3500–4000 m) and it is related to vasogenic cerebral oedema and microhaemorrhages in the CC, documented both in post-mortem autopsies and in non-lethal cases in MRI studies [30, 13]. In addition, in acute mountain sickness, reversible lesions of the splenium of the CC [31] can be observed, attributed to vasogenic or cytotoxic oedema.

Virchow–Robin spaces can be dilated and clearly visible at the level of the CC (Figure 14).

References

1. Gonçalves-Ferreira AJ, Herculano-Carvalho M, Melancia JP, Farias JP, Gomes L. Corpus callosum: microsurgical anatomy and MRI. Surg Radiol Anat 2001;23:409–14.
2. Rakic P, Yakovlev PI. Development of the corpus callosum and cavum septi in man. J Comp Neurol 1968; 132:45–72.
3. Griffiths PD, Batty R, Reeves MJ, Connoly DJ. Imaging the corpus callosum, septum pellucidum and fornix in children: normal anatomy and variations of normality. Neuroradiology 2009;51:337–45.
4. Wolfram-Gabel R, Maillot C, Koritké JG. Vascularization of the corpus callosum in humans. Acta Anat (Basel) 1991; 141:46–50.
5. Wolfram-Gabel R, Maillot C. The venous vascularization of the corpus callosum in man. Surg Radiol Anat 1992; 14:17–21.
6. Taylor M, David AS. Agenesis of the corpus callosum: a United Kingdom series of 56 cases. J Neurol Neurosurg Psychiatry 1998;64:131–4.
7. Wahl M, Strominger Z, Jeremy RJ, Barkouich AJ, Wakahiro M, Sherr EH, et al. Variability of homotopic and heterotopic callosal connectivity in partial agenesis of the corpus callosum: a 3T diffusion tensor imaging and Q-ball tractography study. AJNR Am J Neuroradiol 2009;30:282–9.
8. Rokitansky C. Lehrbuch der Pathologischen anatomie, vol. 2. Vienna, Austria: Braumueller, 1856: 468.

9. Flores-Barragán JM, del Real-Francia MA, Gallardo-Alcañiz MJ. Lipoma of the corpus callosum. Rev Neurol 2008;47:380.
10. Yildiz H, Hakyemez B, Koroglu M, Yesildag A, Baykal B. Intracranial lipomas: importance of localization. Neuroradiology 2006;48:1–7.
11. Lai W, Katirji B. Splenium infarct due to cerebral venous thrombosis. Arch Neurol 2007;64:1540.
12. Kasow DL, Destian S, Braun C, Quintas JC, Kagetsu NJ, Johnson CE. Corpus callosum infarcts with atypical clinical and radiologic presentations. AJNR Am J Neuroradiol 2000;21:1876–80.
13. Kallenberg K, Dehnert C, Dorfler A, Schellinger PD, Bailey DM, Knauth M, et al. Microhemorrhages in nonfatal high-altitude cerebral edema. J Cereb Blood Flow Metab 2008; 28:1635–42.
14. Dietemann JL, Botelho C, Nogueira T, Vargas MI, Audibert C, Abu Eid M, et al. Imaging in acute toxic encephalopathy. J Neuroradiol 2004;31:313–26.
15. Vargas MI, Lenz V, Bin JB, Bogorin A, Abu Eid M, Jacques C, et al. Imagerie par resonance magnetique (IRM) des complications encephaliques de l'alcoolisme. J Radiol 2003;84:369–79.
16. Prilipko O, Delavelle J, Lazeyras F, Seeck M. Reversible Cytotoxic edema in the splenium of the corpus callosum related to antiepileptic treatment: report of two cases and literature review. Epilepsia 2005;46:1633–6.
17. Lin W, Lu C, Lee Y, Wang HC, Lui CC, Cheng YF, et al. White matter damage in carbon monoxide intoxication assessed in vivo using diffusion tensor MR imaging. AJR Am J Neuroradiol 2009;30:1248–55.
18. Fluss J, Ferey S, Menache-Starobinski C, Delavelle J, Van Bogaert P, Vargas MI. Mild influenza-associated encephalopathy/encephalitis with a reversible splenial lesion in a Caucasian child with additional cerebellar features. Eur J Paediatr Neurol 2010;14:97–100.
19. Tanaka Y, Nishida H, Hayashi R, Inuzuka T, Otsuki M. Callosal disconnection syndrome due to acute disseminated encephalomyelitis. Clin Neurol 2006;46:50–4.
20. Kim JH, Choi JY, Koh SB, Lee Y. Reversible splenial abnormality in hypoglycemic encephalopathy. Neuroradiology 2007;49:217–22.
21. Van Hove JL, Kishnani PS, Demaerel P, Kahler SG, Miller C, Jaeken J, et al. Acute hydrocephalus in nonketotic hyperglycemia. Neurology 2000;54:754–6.
22. McComb RD, Pfeiffer RF, Casey JH, Wolcott G, Till DJ. Lateral pontine and extrapontine myelinolysis associated with hypernatremia and hyperglycemia. Clin Neuropathol 1989;8:284–8.
23. Morlan L, Rodriguez E, Gonzalez J, Jimenez-Ortiz C, Escartin P, Liano H. Central pontine myelinolysis following correction of hyponatremia: MRI diagnosis. Eur Neurol 1990;30:149–52.
24. Vargas MI, Kohler R, Lovblad K, Delavelle J. Central pontine myelinolysis: MR findings. Rev Neurol 2009;48: 654–5.
25. Rutgers DR, Fillard P, Paradot G, Tadie M, Lasjaunias P, Ducreux D. Diffusion tensor imaging characteristics of the corpus callosum in mild, moderate and severe traumatic brain injury. Am J Neuroradiol 2008;29:1730–5.
26. Shiramizu H, Masuko A, Ishizaka H, Shibata M, Atsumi I, Osada T, et al. Mechanism of injury to the corpus callosum, with particular reference to the anatomical relationship between site of injury and adjacent brain structures. Neurol Med Chir 2008;48:1–7.
27. Marquez de la Plata C, Ardelean A, Koovakkatu D, Srinivasan P, Miller A, Phuong G, et al. Magnetic resonance imaging of diffuse axonal injury: quantitative assessment of white matter lesion volume.
J Neurotrauma 2007;24:591–8.
28. Wang JY, Bakhadirou K, Devous MD Sr, Abdi H, Moore C. Diffusion tensor tractography of traumatic diffuse axonal injury. Arch Neurol 2008;65:337–45.
29. Zacharia TT, Law M, Naidich TP, Leeds NE. Central nervous system lymphoma characterization by diffusion-weighted imaging and MR spectroscopy. J Neuroimaging 2008;18940:411–17.
30. Hackett PH, Yarnell PR, Hill R, Reynard K, Heit J, McCormick J. High-altitude cerebral edema evaluated with magnetic resonance imaging: clinical correlation and pathophysiology. JAMA 1998;280:1920–5.
31. Johmura Y, Takahashi T, Kuroiwa Y. Acute mountain sickness with reversible vasospasm. J Neurol Sci 2007;263: 174–6.